

## Improvement of the dosimetric properties of chemical-vapor-deposited diamond films by neutron irradiation

Mara Bruzzi,<sup>a)</sup> David Menichelli, and Silvia Pini  
*Dipartimento di Energetica, Via S. Marta, 3, I-50139, Florence, Italy*  
*and INFN, Via G. Sansone, 1, I-50018 Sesto Fiorentino, Italy*

Marta Bucciolini  
*Dipartimento di Fisiopatologia Clinica, Firenze, Italy*  
*and INFN, Via G. Sansone, 1, I-50018 Sesto Fiorentino, Italy*

József Mólnar and András Fenyvesi  
*Institute of Nuclear Research of the Hungarian Academy of Sciences (ATOMKI), Bem tér 18/c.,*  
*P.O. Box 51, H-4001 Debrecen, Hungary*

(Received 13 March 2002; accepted for publication 6 May 2002)

The performance of chemical-vapor-deposited (CVD) diamond films as on-line dosimeters has been substantially improved after irradiation with fast neutrons up to a fluence of  $5 \times 10^{14}$  n/cm<sup>2</sup>. This is correlated to a decrease of more than one order of magnitude in the concentration of deep levels with activation energy in the range 0.9–1.4 eV, as observed by thermally stimulated current and photoinduced current transient spectroscopy. As a consequence, a fast and reproducible dynamic response is observed during irradiation with a 6 MV photon beam from linear accelerator and with a Co<sup>60</sup> source. A quasilinear dependence of the current on the dose rate is obtained in the range of interest for clinical applications (0.1–10 Gy/min). The resulting sensitivity is definitely higher than that of standard ionization chambers, and compares favorably with those of standard silicon dosimeters and of best-quality natural and CVD diamond devices. © 2002 American Institute of Physics. [DOI: 10.1063/1.1491014]

Many outstanding properties of diamond, in particular soft-tissue equivalence, chemical inertness, nontoxicity and radiation hardness, make this material extremely appealing for clinical dosimetry.<sup>1–3</sup> On-line dosimeters made with natural diamond are already commercially available but extremely expensive and rare due to the difficulty in selecting stones with the proper dosimetric characteristics. Chemical-vapor-deposited (CVD) diamond films have been recently proposed in their stead, due to the potential low cost of this material. One crucial problem still unsolved is the CVD diamond doping recipe required to optimize the performance of such devices. It is well known that a quasi-uniform distribution of deep levels is needed to ensure the linear response of the current signal as a function of the dose rate;<sup>4</sup> unfortunately, a high concentration of deep levels might also lead to a worsening of the device transport properties. The bulk of undoped CVD diamond films is characterized by a complexly structured distribution of traps giving rise to many active energy levels. Luminescence spectra are dominated by the broad A band,<sup>5</sup> placed near 3 eV, now related to defects (possibly *sp*<sup>2</sup>-like structures) at dislocations and grain boundaries.<sup>6</sup> However, electrical properties at room temperature are mainly influenced by shallower levels, below 1.5 eV, due to incorporated impurities or correlated to extended defects at grain boundaries.<sup>7,8</sup> These traps can be effective in reducing the carrier lifetimes and, consequently, in worsen-

ing the sensitivity, the dynamic response, and the reproducibility of the device during exposure to the radiotherapy beams.<sup>9</sup>

In this work, we demonstrate that it is possible to significantly improve the dosimetric performance of CVD diamond films by opportunely tailoring the deep level distribution through a preirradiation stage with fast neutrons at high fluence levels. A commercial CVD diamond film with  $1 \times 1$  cm<sup>2</sup> area and 600  $\mu$ m thickness, equipped with Cr/Au ohmic contacts (5 mm diameter) has been irradiated at ATOMKI, Debrecen, Hungary, using fast neutrons produced by 16 MeV protons in a 3 mm thick beryllium target and up to a fluence of  $5 \times 10^{14}$  n/cm<sup>2</sup>. The neutron energy spectrum is monotonically decreasing in the range from 0.1 MeV to about 15 MeV; for higher energies a sharp cutoff occurs.<sup>10</sup> Deep levels before and after neutron irradiation (NI) have been investigated by means of thermally stimulated currents (TSC) and photoinduced current transient spectroscopy (PICTS) using a xenon lamp which generates pulses of 0.1 J and 2  $\mu$ s duration, covering the wavelength range 200–1000 nm, with a peak at 300 nm. The TSC spectra, measured before and after NI, exhibit a broad line peaked at  $\sim 520$  K, as shown in Fig. 1. A detailed investigation revealed that this dominant feature is due to the emission from different deep levels.<sup>11</sup> At least four components are needed to fit the experimental results. The best fit is obtained using four deep levels (Nos. 1–4) characterized by activation energies in the range 0.9–1.4 eV, small capture cross sections ( $10^{-17}$ – $10^{-19}$  cm<sup>2</sup>) and total concentration  $N_t \approx 10^{19}$  cm<sup>-3</sup>. Illumination with the Xe lamp does not ensure a complete trap priming; thus, in order to completely saturate

<sup>a)</sup>Author to whom correspondence should be addressed; electronic mail: bruzzi@fi.infn.it

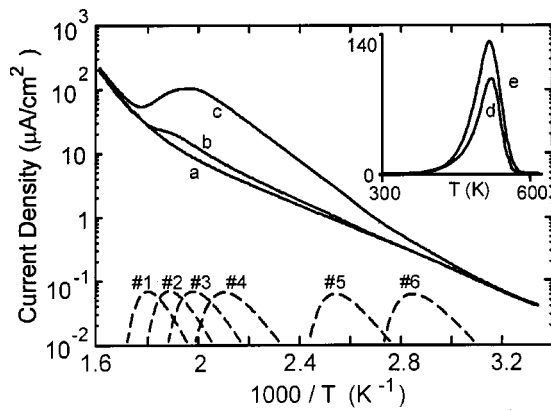


FIG. 1. TSC measurements performed with heating rate  $\beta=0.15$  K/s and  $V_{\text{bias}}=100$  V. The background current (a) is measured without excitation. The other curves in the main plot correspond to measurements performed after a 30 min excitation using the Xe lamp, before (c) and after (b) NI. The contributions of fit components Nos. 1–6, calculated with arbitrary amplitudes, are shown in the bottom (dashed lines) for comparison. The spectra in the inset have been measured after a priming with a  $\text{Co}^{60}$   $\gamma$ -source, up to a dose of 8 Gy; the signal measured after NI (d) is multiplied by ten for better comparison with the spectrum measured before NI (e).

the dominant levels, the sample has been irradiated with the  $\text{Co}^{60}$  source up to a dose of 8 Gy. The resulting TSC spectra are plotted in the inset of Fig. 1, showing that the spectral amplitude is reduced by a factor 20–30 after NI. Some defects activate near room temperature, generating a spectral contribution in the range 300–400 K. The total concentration of these traps before NI was  $N_t \approx 10^{16} \text{ cm}^{-3}$ , but after NI they are no longer observable by TSC. They have been also studied by PICTS, which offers higher sensitivity and resolution than TSC: Results are shown in Fig. 2. The PICTS spectra is calculated as  $S(T) = J(t_2, T) - J(t_1, T)$ ;  $J(t, T)$  denotes the current density transient at the temperature  $T$ . We used  $t_1 = 100 \mu\text{s}$ ,  $t_2 = 400 \mu\text{s}$ , a bias  $V_{\text{bias}} = 50$  V, and a heating rate  $\beta = 0.07$  K/s, slow enough not to affect the spectrum shape. Two deep levels (Nos. 5 and 6) with energy  $\approx 1.2$  eV and very large cross sections ( $\sim 10^{-13} \text{ cm}^2$ ) can partially account for this spectral feature, together with a shallower level, No. 7 ( $E = 0.39$  eV,  $\sigma = 3.2 \times 10^{-19} \text{ cm}^2$ ). The signal amplitude, and thus the concentration of deep levels Nos. 5–7, are reduced about one order of magnitude after NI.

The reduction of the deep levels concentration deter-

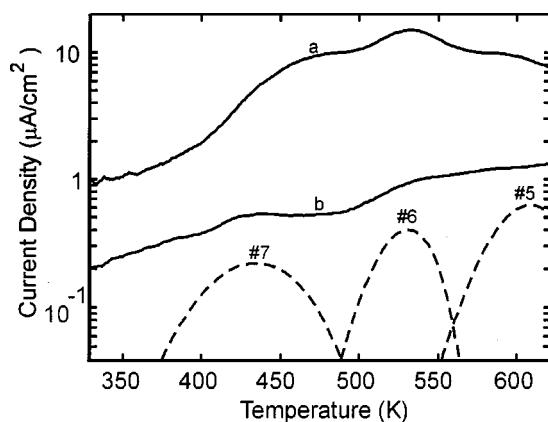


FIG. 2. PICTS spectra measured before (a) and after (b) NI. The calculated spectral lines corresponding to deep levels Nos. 5–7 are reported in the bottom (dashed lines), with arbitrary amplitude, for comparison.

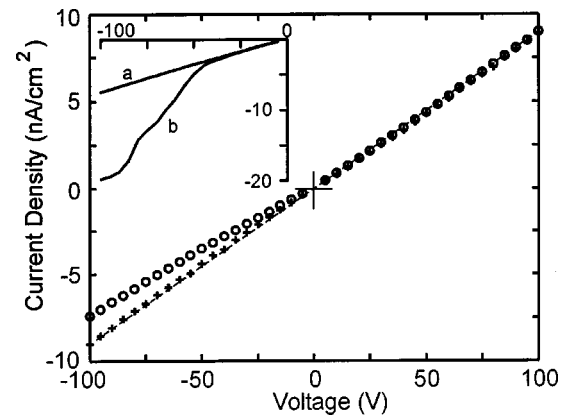


FIG. 3.  $I$ - $V$  characteristics before (circles) and after (crosses) NI. The dashed lines represent the fit of the characteristic after neutron irradiation, corresponding to a resistivity  $1.8 \times 10^{11} \Omega \text{ cm}$ . Two curves measured before NI are shown in the inset. Curve (a) is identical to the curve marked with circles in the main plot, and is compared with the characteristic measured after exposure to Xe lamp (curve b).

mines a general stabilization of the current response. As shown in Fig. 3, before NI, the current–voltage ( $I$ - $V$ ) characteristic is nonsymmetric with respect to  $V_{\text{bias}}=0$ , and shows a linear behavior only for positive biases. This is probably due to polarization effects.<sup>12,13</sup> After NI, the  $I$ - $V$  curve becomes almost linear and symmetric, denoting a good ohmic behavior, with a resistivity of about  $1.8 \times 10^{11} \Omega \text{ cm}$ . In the inset, the characteristic measured before NI is compared with the same characteristic obtained after a 30 min exposure to the xenon lamp and a 30 min de-excitation at room temperature. After illumination, the current grows, and the  $I$ - $V$  curve becomes highly nonlinear, putting into evidence the occurrence of polarization effects. The initial  $I$ - $V$  behavior is recovered after 20 h annealing at room temperature, or after heating the sample at 650 K.

The dosimetric characterization of the sample was carried out at the radiotherapy unit of Dipartimento di Fisiopatologia Clinica of Florence. During exposure, the sample was placed in a cylindrical polymethylmethacrylate housing and biased with  $V_{\text{bias}} = 100$  V. The current response of the sample under exposure to a  $\text{Co}^{60}$  source (dose rate  $D_r = 0.2$  Gy/min) is shown in Fig. 4. To passivate the deeper

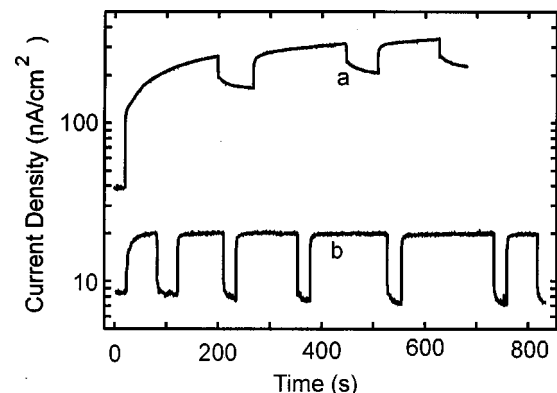


FIG. 4. Current response of the CVD diamond during room temperature exposure to a  $\text{Co}^{60}$   $\gamma$ -source measured (a) before (as grown) and (b) after NI. The source has been switched on and off several times to test the dynamic response of the sample. The applied voltage is 100 V, the dose rate is 0.3 Gy/min.

traps, the sample has been  $\gamma$ -irradiated up to a dose of 20 Gy before measurements. Before NI, the current under  $\gamma$  exposure is steadily increasing during time and, when the beam is switched off, the current shows a slow decay. After NI, the intensity of the on-line current is lowered by one order of magnitude, but the dynamic response is heavily improved. The signal is well reproducible after several irradiation cycles, achieving a stable value within a few seconds. The charge released over each irradiation cycle grows linearly with the absorbed dose, determining a sensitivity of about 45 nC/(Gym<sup>3</sup>). This value is definitely higher than the sensitivity of ionization chambers, and compares favorably with those of standard silicon dosimeters and best-quality CVD and natural diamond devices.<sup>14,15</sup>

The current response as a function of the dose rate has been studied using the Co<sup>60</sup> source and a 6 MV photon radiotherapy beam from a linear accelerator in the range 0.1–10 Gy/min. Results have been fitted to the standard relationship for on-line dosimeters:  $I = I_0 + RD_r^\Delta$ , with  $\Delta = 0.9$ . The quasilinear dependence of the current response with the dose rate suggests that, after NI, a significant residual trap concentration is still present in the material. The microscopic mechanism which causes the radiation-induced removal of the 0.9–1.4 eV levels is presently not clear. Neutron irradiation generates vacancy–interstitial pairs in the material bulk. The capture of mobile self-interstitial at extended defects or grain boundaries has been invoked to explain the decreased intensity of the 2.156 eV luminescence line after neutron irradiation.<sup>16</sup> This explanation was based on the assumption that the self-interstitial is mobile at room temperature. However, recent studies<sup>17</sup> indicate that the self-interstitial is not mobile below 700 K. Vacancy is not mobile at room temperature, as well.<sup>18</sup> Defects related to vacancy are created by neutron irradiation, giving rise to the well known *GR* and *ND* absorption bands.<sup>19,20</sup> The shallower vibronic system *GR1*, which is related to neutral vacancy, is characterized by a zero-phonon line at 1.67 eV; the *GR2* to *GR8* lines are localized between 2.8 and 3.0 eV, while the *ND1* system, associated with the vacancy in negative state, has a zero-phonon line at 3.15 eV. *GR2–8* and *ND1* transitions are associated with photoconductivity,<sup>19</sup> but are not detectable by TSC and PICTS in the temperature range investigated in this work, due to their high activation energy. For the same reason, they should produce a negligible effect on the dynamic response of the device operating at room temperature. Since vacancies and interstitials are not mobile at room temperature, their reaction with existing defects at grain boundaries can not explain the decrease of the TSC and PICTS signals after NI. Nevertheless, the vacancy could act as a deep trap or recombination center for carriers. The deep

energy levels created in large concentration by NI could interact with the existing 0.9–1.4 eV levels, significantly reducing their filling under excitation. Moreover, if 0.9–1.4 eV levels are related to extended defects, structural changes subsequent to the direct collision between defects and neutrons might occur.

Our results demonstrate that fast neutron irradiation at high fluence levels can be a very useful tool to optimize the performance of CVD diamond devices, through the controlled tailoring of the deep level distribution in the material bulk. This opens the way for the development of low cost, high-quality CVD diamond on-line dosimeters for clinical applications in radiotherapy.

The authors wish to thank M. Scaringella for technical support. This work has been carried out in the framework of the RD42 (CERN) and of the CANDIDO (INFN) collaborations. The neutron irradiation at ATOMKI was supported in part by the Hungarian Scientific Research Fund (OTKA) (Contract No. T T026184).

<sup>1</sup>R. J. Keddy, T. L. Nam, and R. C. Burns, *Phys. Med. Biol.* **32**, 751 (1987).

<sup>2</sup>E. A. Burgemeister, *Physica B* **11**, 319 (1981).

<sup>3</sup>J. Barthe, *Nucl. Instrum. Methods Phys. Res. B* **184**, 158 (2001).

<sup>4</sup>J. F. Fowler, in *Radiation Dosimetry*, edited by F. H. Attix and W. C. Roesch (Academic, New York, 1966), Vol. 2, pp. 291–322.

<sup>5</sup>J. Ruan, K. Kobashi, and W. J. Choyko, *Appl. Phys. Lett.* **60**, 3138 (1992).

<sup>6</sup>D. Takeuchi, H. Watanabe, S. Yamanaka, and H. Okushi, *Phys. Rev. B* **63**, 245328 (2001).

<sup>7</sup>E. Vittone, C. Manfredotti, F. Fizzotti, A. LoGiudice, P. Polesello, and V. Ralchenko, *Diamond Relat. Mater.* **8**, 1234 (1999).

<sup>8</sup>D. Tromson, A. Brambilla, P. Bergonzo, A. Mas, C. Hordequin, C. Mer, and F. Foulon, *J. Appl. Phys.* **90**, 1608 (2001).

<sup>9</sup>P. J. Sellin, M. B. H. Breese, A. P. Knights, L. C. Alves, R. S. Sussmann, and A. J. Whitehead, *Appl. Phys. Lett.* **77**, 913 (2000).

<sup>10</sup>M. A. Lone, C. B. Bigham, J. S. Fraser, H. R. Schneider, T. K. Alexander, A. J. Ferguson, and A. B. McDonald, *Nucl. Phys. A* **143**, 331 (1977).

<sup>11</sup>M. Bruzzi, L. Lombardi, D. Menichelli, and S. Sciortino, *J. Appl. Phys.* **91**, 5765 (2002).

<sup>12</sup>M. Marinelli, E. Milani, A. Paoletti, A. Tucciarone, G. Verona Rinati, M. Angelone, and M. Pillon, *Diamond Relat. Mater.* **10**, 645 (2001).

<sup>13</sup>B. Gan, J. Ahn Rusli, Q. Zhang, S. F. Yoon, V. A. Ligatchev, J. Yu, K. Chew, and Q. F. Huang, *J. Appl. Phys.* **89**, 5747 (2001).

<sup>14</sup>C. De Angelis, S. Onori, M. Pacilio, G. A. P. Cirrone, G. Cuttone, L. Raffaele, M. Bucciolini, and S. Mazzocchi, *Med. Phys.* **29**, 248 (2002).

<sup>15</sup>C. M. Buttar, R. Airey, J. Conway, G. Hill, S. Ramkumar, G. Scarsbrook, R. S. Sussmann, S. Walker, and A. Whitehead, *Diamond Relat. Mater.* **9**, 965 (2000).

<sup>16</sup>L. Allers, A. S. Howard, J. F. Hassard, and A. Mainwood, *Diamond Relat. Mater.* **6**, 353 (1997).

<sup>17</sup>D. C. Hunt, D. J. Twitchen, M. E. Newton, J. M. Baker, T. R. Anthony, W. F. Banholzer, and S. S. Vagarali, *Phys. Rev. B* **61**, 3863 (2000).

<sup>18</sup>G. Davies, S. C. Lawson, A. T. Collins, A. Mainwood, and S. J. Sharp, *Phys. Rev. B* **46**, 13157 (1992).

<sup>19</sup>J. Walker, *Rep. Prog. Phys.* **42**, 1605 (1979).

<sup>20</sup>J. E. Lowther, *Phys. Rev. B* **48**, 11592 (1993).